1984

A Generalized Performance Computer Program for Oil Flooded Twin-Screw Compressors

P. J. Singh

G. C. Patel

A GENERALIZED PERFORMANCE COMPUTER PROGRAM FOR OIL FLOODED TWIN-SCREW COMPRESSORS

Pawan J. Singh and Ghanshyam C. Patel
Ingersoll-Rand Research, Inc.
Princeton, NJ

1. ABSTRACT

A general purpose computer program to predict performance of oil-flooded twin-screw compressors has been written. The program accounts for all leakages, viscous shear losses, oil cooling, and inlet and discharge losses. It uses some empirical coefficients which have been developed based on extensive test data. These coefficients are used to define leakage blockage, shear losses, and heat transfer due to the presence of oil. The program's results have been extensively checked against test data and shown to give a good agreement over a wide tip speed range and for several different machines having different rotor profiles and number of lobe combinations.

This paper describes the theory used in the program and then presents some results to show comparison between program predictions and test data. The paper also enumerates the performance losses due to various sources for a better understanding of the compressor performance.

2. INTRODUCTION

Rotary helical twin screw compressors are mainly used in industry for gas compression and refrigeration. The selection of a particular compressor size for a given application generally depends on the manufacturer's past experience. However, new applications and recent emphasis on performance improvement due to high energy cost require that machine performance be much better understood and be predictable.

Several investigators (2-5) have published methods for analyzing screw compressor performance with varying levels of mathematical sophistication. Most of the results presented in these investigations are for the common SRM type compressors. The invention and use of many new rotor end profiles require that the performance prediction tool not be limited to a certain profile. Reference 1 details a computer-assisted technique for generating and analyzing new profiles. The most important step in determining the merits of a new profile is to be able to predict its performance relative to other profiles in a compressor application. Besides the profile shape, a designer can select a number of other variables such as wrap angle, L/D ratio, built-in pressure ratio, oil injection quantity, tip-speed or rpm, and all of these have a significant effect on the performance. The performance prediction method should therefore be valid for most profiles and a broad range of design and operating conditions. This paper presents such a generalized performance prediction computer program for oil-flooded or wet screw compressors.

3. METHOD OVERVIEW AND ASSUMPTIONS

The program follows one compressor cavity (one male and one female lobe) from its inception at $\theta = 0$ to fill-up through the inlet port, and then to compression and discharge until its extinction at $\theta = (360(1+1/Nm)+\text{wrap angle})$ degrees. The pressure in this cavity is computed from the mass and energy conservation (First Law of Thermodynamics) equations along with computation of flow through inlet and discharge ports and various leakage flows. These equations are expressed in the form of a set of differential equations which are simultaneously solved at small integration steps using the fourth order Runge-Kutta method. The gas power or power required only for the compression of gas is determined by calculations P-V work done for one cavity and multiplying it by the number of cavities formed per unit time. Viscous shear losses and mechanical power losses are then added to obtain BHP. Compressor capacity is determined by integrating the discharge mass flow over the discharge process.

The program makes certain assumptions which are not restrictive for general screw compressor applications but are stated below for clarity:

o The fluid is a perfect gas with constant specific heat C_p.

o Oil and gas are assumed to be separate fluids. Oil-gas interaction takes place only through heat transfer.

o Oil-gas heat transfer is assumed to be proportional to the chamber volume and oil-gas temperature difference.

o Average clearances are used in determining leakage flows. It is assumed that such averaging gives a good representation of the actual leakage flows.

o Unsteady flow fluid inertia effects at the inlet and discharge ports are approximated by pressure loss terms as explained later.

The method accounts for each capacity loss explicity and these values are printed out by the program. Similarly BHP is also divided into gas power, different viscous shear losses, mechanical and bearing power losses, and discharge port loss.

4. THEORY

4.1 Thermodynamic Model

The thermodynamic model used in the program closely parallels the one reported in Reference 6 for vane compressor applications. It is briefly restated here for the sake of completeness. The symbols used in the following equations are described in the Appendix.

The sketch below schematically shows a compressor cavity at time t and a small time step Δt later at $t+\Delta t$. At time t, the mass in the cavity is m(t); dm_i and dm_o are small masses which will flow into and out of the cavity respectively in time increment Δt. This inflow or outflow could result from flow in either direction through the inlet port or the discharge port, or leakages through various clearances.

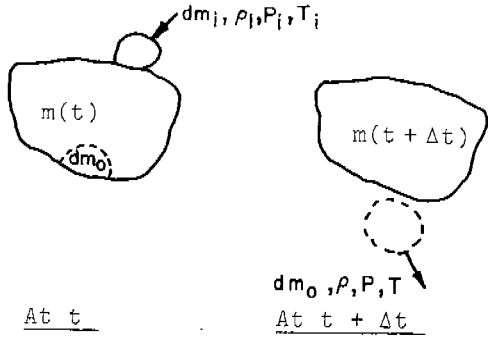

For a system as shown we can apply the First Law of Thermodynamics in the time interval Δt. Since we have assumed perfect gas,

$$dq = dE + dW \tag{1}$$

$$dE = C_v \{ m dT + \Sigma (T - T_i) dm_i \} \tag{2}$$

The work term dW can be written as,

$$dW = PdV - \Sigma \frac{P_i}{\rho_i} dm_i + \frac{P}{\rho} dm_o \tag{3}$$

Combining (1), (2) and (3),

$$dQ = C_v \{ m dt + \Sigma (T - T_i) dm_i \} + P dv - \Sigma \frac{P_i}{\rho_i} dm_i + \frac{P}{\rho} dm_o \tag{4}$$

The mass relationship at time t and $t+\Delta t$ can be expressed as,

$$m(t+\Delta t) = m(t) + dm_i - dm_o \tag{5}$$

Introducing time derivatives with the definitions

$$\dot{Q} = \frac{dQ}{dt}; \quad \dot{m}_i = \frac{dm}{dt}; \quad \dot{m}_o = \frac{dm_o}{dt}; \quad \dot{m} = \frac{dm}{dt}$$

Then, from (5)

$$\dot{m} = \dot{m}_i - \dot{m}_o \tag{6}$$

The time can be eliminated for rotation angle θ by the definition,

$$dt = d\theta / \omega \tag{7}$$

Using (6) and the perfect gas law, we can reduce (4) to a useful form,

$$\frac{dP}{d\theta} = \frac{\gamma - 1}{\omega V} \dot{Q} - \frac{\gamma P}{V} \frac{dV}{d\theta} - \frac{\gamma P}{\rho \omega V} \dot{m}_o + \frac{\gamma}{\omega V} \Sigma \frac{P_i}{\rho_i} \dot{m}_i \tag{8}$$

A more expanded version of the above equation is used in the program to calculate pressure. The equation (8) also differs in form from the relationship used by most other investigators. However (8) brings out the physics of the compression process more clearly. For example, (8) can be rewritten as:

$$\frac{d}{d\theta} (PV^\gamma) = \frac{\gamma V^{\gamma - 1}}{\omega} \{ \frac{\gamma - 1}{V} \dot{Q} + \Sigma \frac{P_i}{\rho_i} \dot{m}_i - \frac{P}{\rho} \dot{m}_o \} \tag{9}$$

In the absence of heat transfer ($\dot{Q} = 0$),

$$\frac{d}{d\theta} (PV^\gamma) = \frac{\gamma V^{\gamma - 1}}{\omega} \{ \Sigma P_i \dot{V}_i - P_o \dot{V}_o \} \tag{10}$$

where $\dot{V}_i$ and $\dot{V}_o$ are inflow and outflow volume rates. If $\dot{V}_i$ and $\dot{V}_o$ are zero (closed cavity with no leakages), (10) reduces to adiabatic process,

$$PV^{\gamma} = \text{Constant} \qquad (11)$$

Many investigators use (11) or a similar polytropic process for the compression phase. However, (10) shows that in the presence of leakage flow, this assumption is not strictly valid. In reality, if we ignore heat transfer effects which are generally not dominant in screw compressors, the pressure rises more rapidy than adiabatic process during early stages of compression when incoming leakage flow is dominant ($P_i\dot{V}_i > P\dot{V}_o$ in (10)), and less rapidly during later stages when $P\dot{V}_o < P_i\dot{V}_i$.

This affects the pressure distribution and thus changes compressor torque variation. The total compression work can be approximated by (11) with the selection of a proper polytropic constant.

As another simplification, if the incoming flow during the inlet process follows the cavity volume change rate and there are no leakages, (10) reduces to,

$$\frac{dp}{d\theta} = 0 \text{ or } P = \text{Constant} \qquad (12)$$

The pressure in the cavity, as expected, remains constant. The same applies for the discharge process.

4.2 Leakage Flow Computation

The program accounts for several sources of leakage flow into and out of the cavity as enumerated below:

o Leakage through the rotor-to-rotor clearance called interlobe leakage.

o Leakage through the rotor tip - housing clearance both for leading and lagging cavities.

o Leakage through discharge and clearance both for leading and lagging cavities.

o Leakage through blow-hole both for leading and lagging cavities.

These leakages are expressed by $\dot{m}_i$ and $\dot{m}_o$ terms in (9) and are calculated using the following relationship.

$$\dot{m} = CA\sqrt{2g\rho_1 P_1(1-P_2/P_1)}\ \{1-\frac{3}{4\gamma}(1-\frac{P_2}{P_1})\} \qquad (13)$$

For choked flow or near-choked flow conditions, $\overline{P_2/P_1}$ in the last term in (13) is substituted by a constant (For air, $P_2/P_1 = 0.65$ when $P_2/P_1 < 0.65$). Subscripts 1 and 2 refer to the upstream and downstream conditions respectively. The equation (13) is a simplified form of the usual compressible flow equation for an orifice and accurate to within 2%-3% over the usual operating range.

The term A in (13) defines an equivalent orifice area which results in the same leakage flow as through a particular clearance in the compressor. A is determined by multiplying leakage line length with an average gap for each type of leakage. The average gap is determined from the actual clearance measurements in the compressor. However this gap may vary along different points on the rotor profile. The user then has to estimate a mean value for the gap. The leakage line lengths are determined from Reference 1.

The term C in (13) defines a discharge coefficient empirically selected to account for the presence of oil. Oil injection complicates the analysis in many ways. The oil blocks the leakage paths but to a varying degree according to the leakage type. Tests have shown that the injected oil rapidly centrifuges out to the housing where it is very effective in blocking leakage through rotor tip clearance. Some of the oil also leaks through interlobe and end clearance thus reducing leakage flow through these gaps. The actual blockage depends on the quantity and location of oil injection and the rotor tip speed.

The values of C used in the program vary according to the type of leakage, male rotor tip speed, and quantity of oil injected. These values in the form of equations were developed by matching test data for one compressor with computer predictions over a wide range of operating conditions including tip speed and oil quantity. These equations for C have been used for many other test compressors with good results. These compressors had different profiles, sizes, clearances, and the quantity and viscosity of injected oil.

The test results are reported later in this paper.

4.3 Inlet and Discharge Flow

The mass flow through inlet or discharge ports is calculated using (13) again. The inlet and discharge port area varies withθ and this variation is determined from reference 1. Since a mixture of oil and gas leaves the discharge port, the power loss for the discharge of oil is calculated separately assuming equal velocities for air and oil. In this

manner, discharge port losses due to oil's presence are separated and printed in the program output. Certain other corrections to nominal inlet and discharge pressures are applied to account for a number of factors normally not considered in compressor simulation. Inlet and discharge pressures in tests are generally measured at the respective flanges. However, the cavity pressure during inlet, ignoring pressure drop due to port restriction, may be less than the nominal pressure due to following factors:

o Pressure drop between flange and entry to the inlet port.

o Centrifugal average pressure drop in the cavity because of radial pressure gradient.

o Pressure drop due to axial or radial flow acceleration required to catch up with the cavity tip speed.

Similarly, the intermittent flow at the discharge port induces 'acoustic' pressure pulsations during discharge. The magnitude of these pulsations and the resultant power loss depends on the discharge piping system impedence. Selected runs were made using the discharge process program mentioned in Reference 1 assuming a long, non-reflecting discharge pipe. Based on these runs, the acoustic losses are represented in the form of a discharge pressure correction. This correction is further described in the Appendix.

4.4 Heat Transfer

The basic heat transfer model was previously described in Reference 6 and is summarized here again. It is assumed that all the heat transfer takes place between gas and oil and is given by,

$$\dot{Q} = \dot{Q}_{gas} = HV\ (T_{oil} - T) \qquad (14)$$

H is an empirical constant defined as oil-to-gas heat transfer coefficient per unit volume. Equation (14) assumes that total heat transfer is proportional to the cavity volume. This assumption is based on fully mixed flow with small oil droplets whose surface is proportional to the cavity volume and is much larger than the cavity wall area. Since the oil gas mixture is quite stratified at higher tip speeds, this assumption becomes less valid. Fortunately through the amount of heat transfer at high tip speeds is minimal due to small residence time. In fact, most of the heat transfer in cooling the gas takes place away from the cavity in the discharge pipe.

The oil temperature is determined from an energy balance for the oil in which it is assumed that all dissipated power such as in shear losses goes into heating the oil. Accordingly,

$$\frac{dT_{oil}}{dt} = -\frac{\dot{Q}_{gas} + \Phi_d}{M_{oil}\, C_{oil}} \qquad (15)$$

Thus, at every integration step, the program calculates P, ρ, T for the gas and M_{oil} and T_{oil} for the oil.

4.5 Frictional and Mechanical Losses

Frictional or viscous shear losses result from the presence of oil in small gaps, such as between rotor lobes or rotor tip and housing. The latter loss is generally predominant unless a seal strip is used to minimize the shear area. Shear losses along with discharge port losses become predominant at higher tip speeds where their accurate computation becomes very important. The interlobe shear losses are generally minor since the relative velocities in the vicinity of close gaps are small and the effective shear area is also small. The relationship used to compute these losses are given in the Appendix.

Mechanical power losses were generally assumed to be 2% to 4% of the BHP. Bearing power losses were either calculated outside the program using bearing manufacturer supplied loss procedures or approximated in the program by a user-supplied average friction coefficient.

Additionally, the program also accounts for scavenging orifice losses for those compressors in which the separator oil, along with some gas, is scavenged back to the compressor cavity.

5. COMPARISON WITH TEST DATA

Performance tests on several compressors were run in the laboratory using a dynamometer. The capacity was measured at the discharge end using calibrated ASME orifices of several sizes. The speed, oil flow, pressures and temperatures were measured with appropriate instruments. All the tests were run with a nominal oil injection quantity in compliance with the manufacturer's instructions. The oil quantity remained fixed with change in rpm. The test data was adjusted to a nominal 14.5 psia inlet and 100 or 105 psig discharge. The absolute accuracy of HP or CFM measurements is estimated to be $\pm 2\%$ while the repeatability was shown to be better than $\pm 1\%$.

The tested compressors are labeled as Compressor 1 to 5 and they include the machines produced by the authors' company as well as competitive machines purchased for testing. They cover a wide spectrum of sizes (100-300 mm), L/D ratios (1.5 to 1.9), interlobe clearances (1-3 mils), rotor-tip clearances (3-8 mils), number of male or female rotor lobes (4 to 6). They include at least three entirely different profiles. The compressors are not explicity identified because the purpose of this paper is to demonstrate that a satisfactory generalized performance prediction capability has been achieved and not to divert attention to relative performance of different compressors. It must be stressed that the actual test numbers, such as BHP/100 CFM, are not very meaningful since the compressor clearances vary for each test. For the same reason, empirical coefficients used in the computer runs are not given.

Figure 1 to 5 show BHP/100 CFM and CFM test data and computer predictions for Compressors 1 to 5 over a male rotor tip speed range of 10 to 50 m/sec, and 100 or 105 psig discharge. In some cases, the test data was not available for the whole tip speed range. For all these runs, the empirical coefficients followed the fixed rules built into the program's logic. Compressor 2 shows a different trend for the BHP/100 CFM curve where, unlike other compressors, the curve moves steeply upwards at lower tip speeds. This happens because this particular compressor has larger clearances and has a profile with much larger blow-hole than the others. The program not only gives accurate results but also correctly follows the curve shapes.

Figure 6 gives the results of compressor 1 operating at higher pressure ratio (Pd = 150 psig). The BHP test results are within 2-3% of the computer predictions. Figure 7 summarizes the results of Figure 1 to 5 by plotting measured/calculated CFM and BHP/100 CFM values against tip speed. It shows that the data falls generally within 3% indicated by dashed lines. One point falling out of this range is for very low CFM where the measurement accuracy is suspect.

One of the main objectives of this work was to enhance a designer's understanding of the various types of performance losses. Figures 8 to 12 are derived from performance loss analysis for compressor 1. Figure 8 shows gas power/100 CFM and BHP/100 CFM percentage losses at varying tip speed due to different leakage paths. The figure indicates the percentage gain in performance if a particular leakage source was completely eliminated by assuming the gap to be zero. The BHP loss curve, however, includes shear losses which are based on 1 mil gap since the losses become infinite at zero gap. The leakage losses decrease at higher tip speeds as expected and for this particular case, leakage through rotor tips contributes most gas power loss. However, BHP loss for rotor tip becomes negative at 50 m/sec tip speed, meaning BHP will actually go up if rotor tip clearance is reduced to near-zero because of rapid increase in shear losses. Thus, the program provides a guidance as to the optimum clearances and to the most effective way to achieve performance gain. Figure 9 shows the relative ranking of CFM losses through various leakage paths.

Figure 10 shows specific power vs. tip speed for compressor 1 for various interlobe clearances as predicted by the computer program. It points out to the importance of accurate profile machining with close tolerances. As the interlobe gap increases, the optimum performance point shifts to higher and higher tip speed. In other words, leaky compressors like to run faster. Figure 11 shows the effect of variable rotor tip clearance on compressor 1 indicating that for each tip speed, a particular clearance gives the least BHP/100 CFM value. Figure 12 shows the itemization of power and CFM losses for the same compressor at two tip speeds, which provides a useful quantitative understanding of the losses.

6. CONCLUSIONS

A generalized performance prediction computer program for oil-flooded rotary twin-screw compressors has been presented and shown to give good agreement with test data. It has the following features:

o The program accounts for all reasonable capacity and power losses in a rational manner. Empirical coefficients are used only wherever necessary and these coefficients are shown to have broad applicability.

o The program has been checked against test data for several compressors and shown to match the data within 3%.

o The program enumerates all capacity losses and several types of power losses. This information can be very useful to a designer in improving compressor performance and selecting the right compressor.

ACKNOWLEDGEMENTS

The authors gratefully acknowledge many contributions of A. Sherrill of Ingersoll-Rand (IR) Portable Compressor

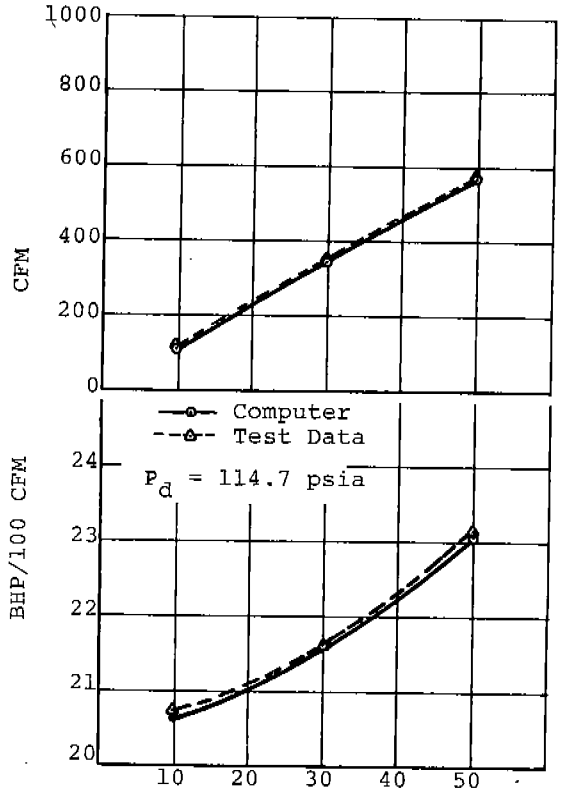

Fig.1. Performance comparison for compressor -1

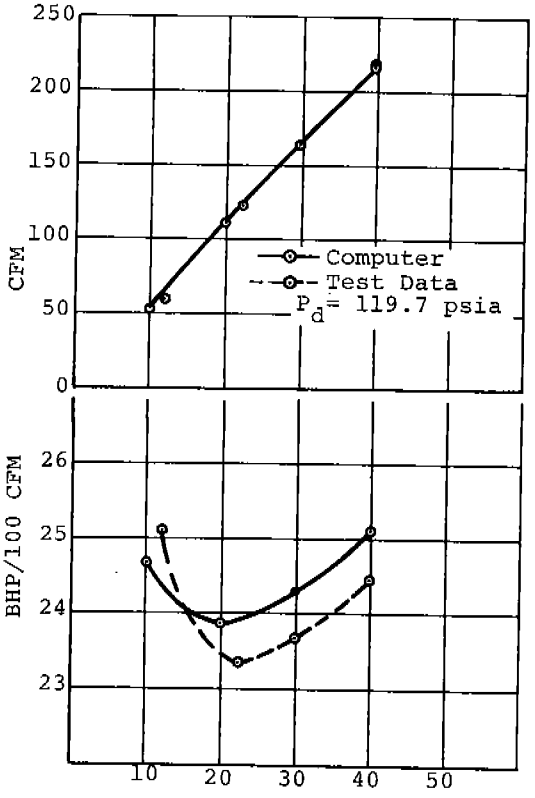

Fig. 2. Performance comparison for compressor -2

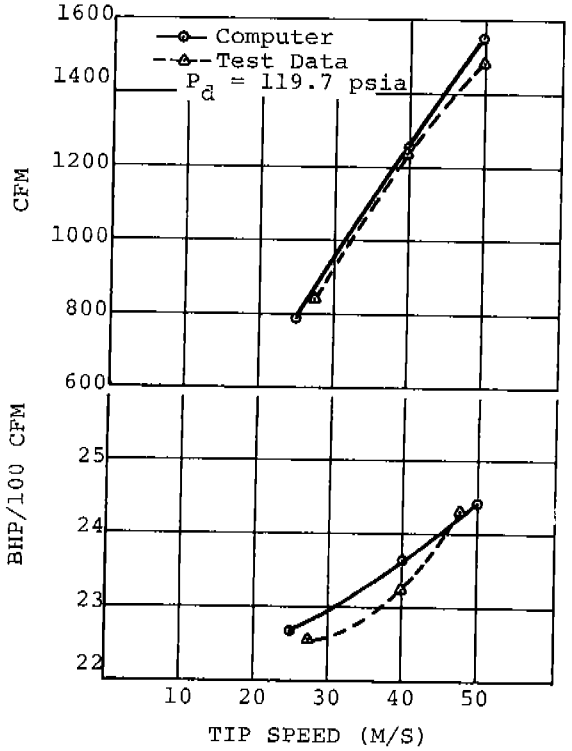

Fig. 3. Performance comparison for compressor -3

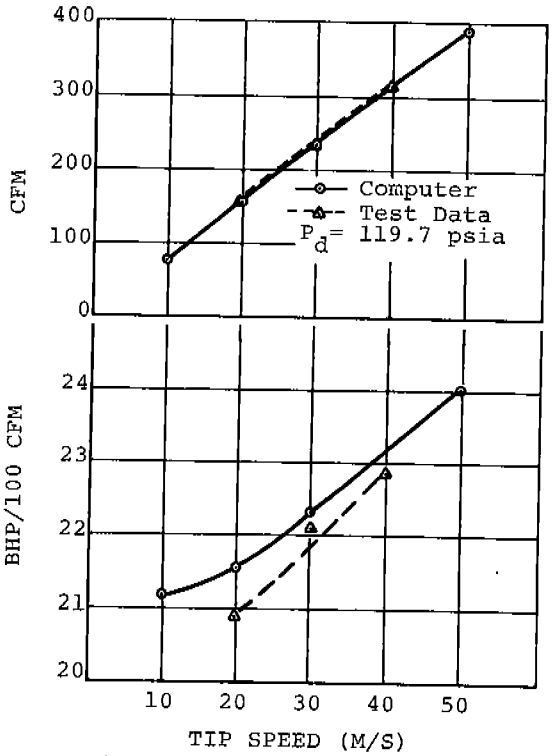

Fig. 4, Performance comparison for compressor -4

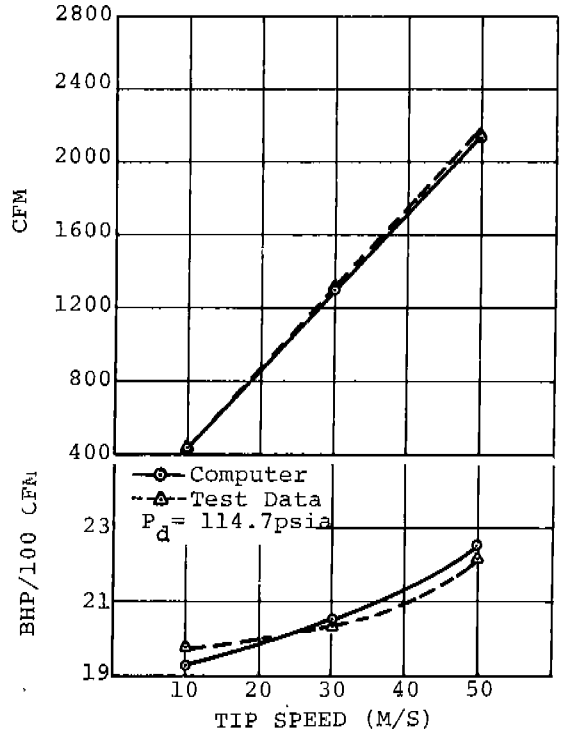

Fig.5. Performance comparison for compressor -5

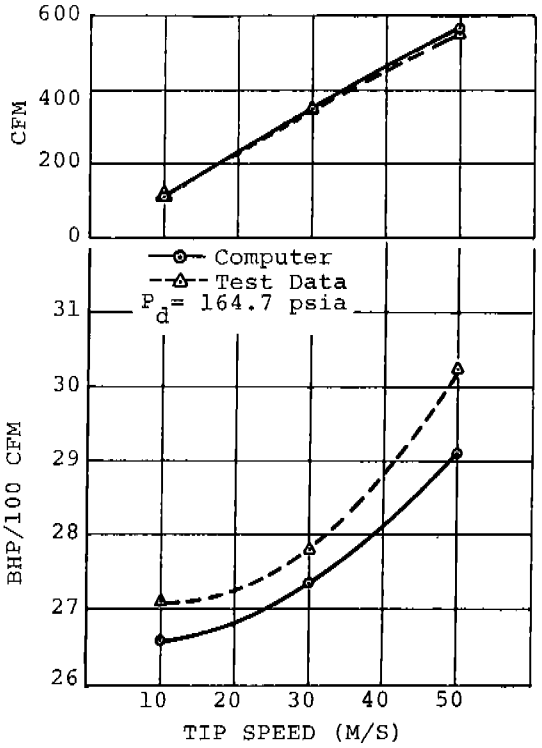

Fig.6. Performance comparison for compressor -6

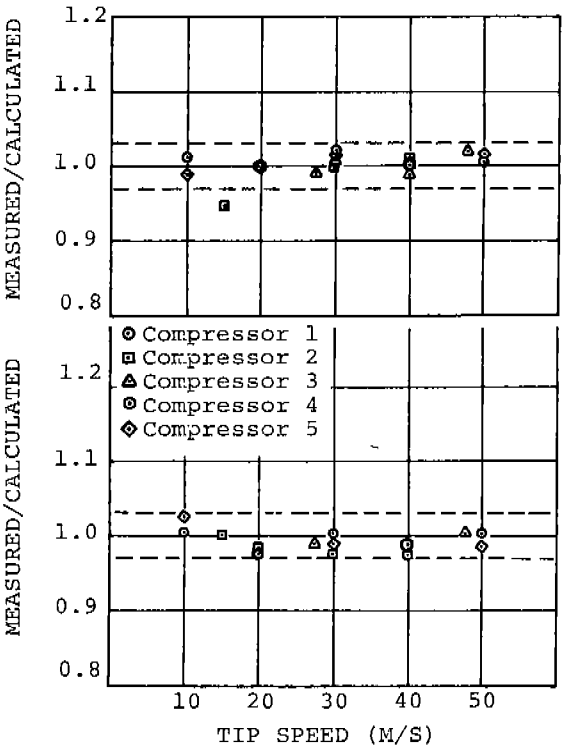

Fig.7. Performance comparison for compressors

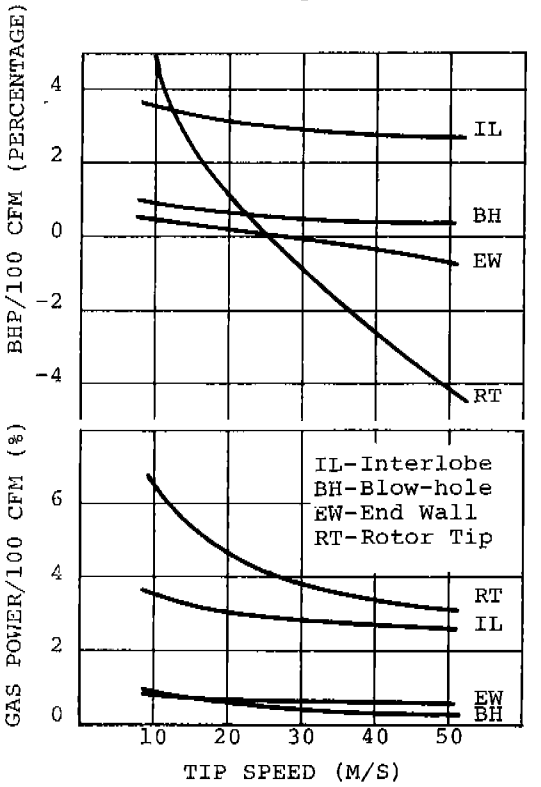

Fig.8. Power losses for various clearances

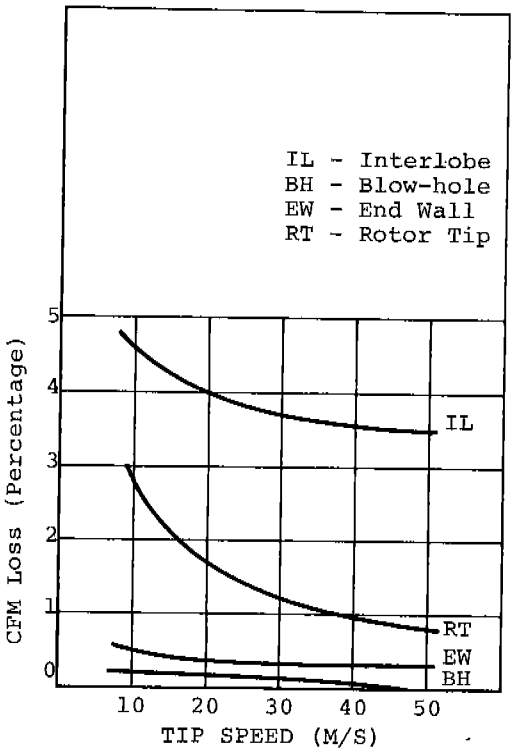

Fig. 9. Flow losses through various clearances for compressor -1

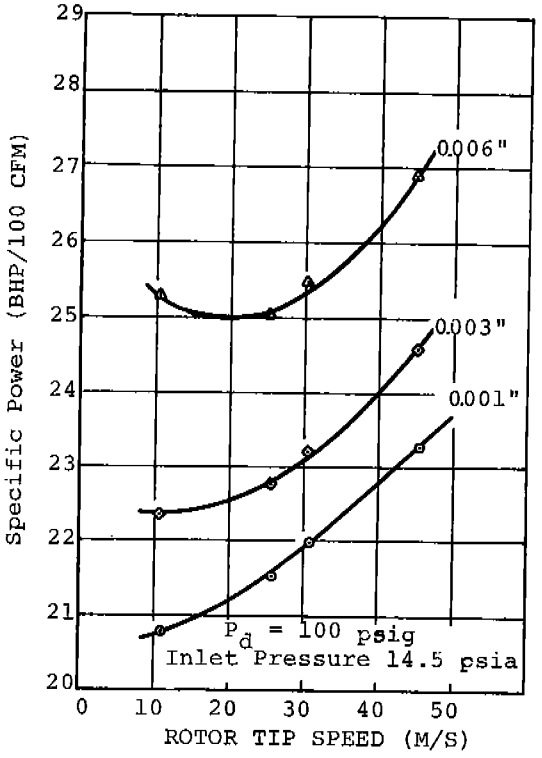

Fig. 10. Performance for various interlobe clearances for compressor -1

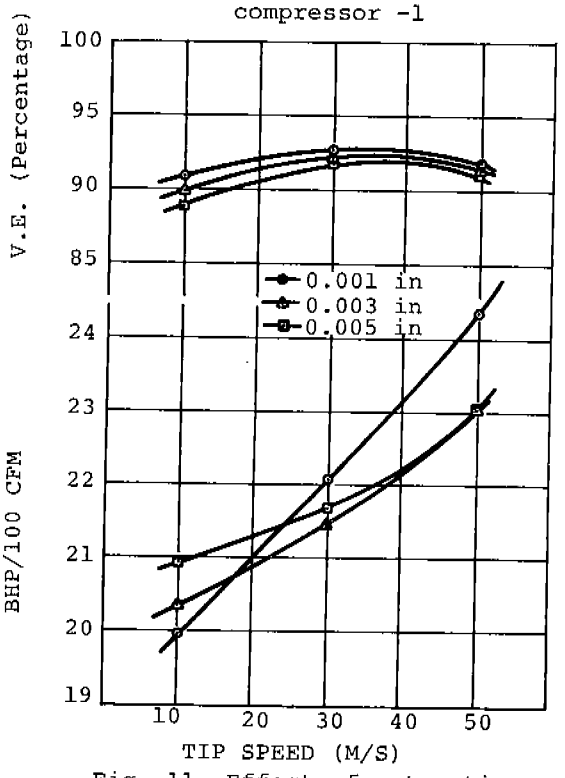

Fig. 11. Effect of rotor tip clearance for compressor -1

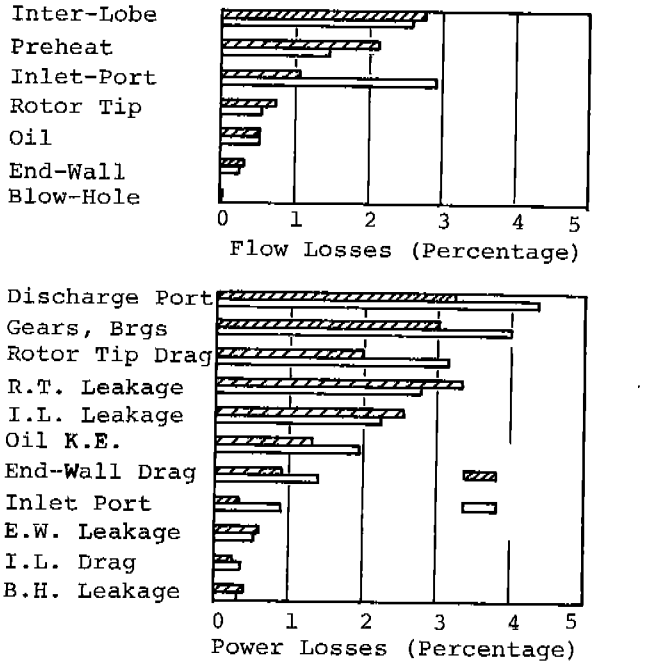

Fig. 12. Apportionment of flow and power losses for compressor -1

Division and J. Bowman and A. Jamieson of IR Rotary Compressor Division in supplying test data and analyzing results, and A. Onuschak of IR Research Center for making most of the computer runs.

APPENDIX

Symbols

A_{min}	Minimum restriction areas in inlet manifold
A_{mt}	Effective male rotor tip shear area
A_{ft}	Effective female rotor tip shear area
C_p, C_v	Specific heat of oil at constant pressure or volume
C_{oil}	Specific heat of oil
dm_i	Incremental mass flow into cavity
dm_o	Incremental mass flow out of cavity
D_m, D_f	Male, female rotor diameter
D_{im}, D_{if}	Male, female rotor root diameter
D_{sm}, D_{sf}	Male, female discharge end shaft diameter
E	Internal energy of the system
L	Rotor length
L/D	Length/male rotor diameter ratio
h_{rt}	Average rotor tip clearance
h_{ew}	Average end wall clearance
h_{il}	Average interlobe clearance
K_{0--7}	Orifice and other empirical coefficients including constants
m	Mass in the cavity at instant t
m_i	Mass flow rate into the cavity
m_o	Mass flow rate out of the cavity
M_{oil}	Oil mass flow rate
N_m, N_f	Number of male, female lobes
P	Pressure in the cavity
P_i	Pressure of the incoming gas
P_d	Nominal discharge pressure
Q_f	Capacity at inlet conditions
Q	Overall heat transfer
Q_{gas}	Heat transfer to or from gas
R	Lobe depth $((D_m - D_{im})/2)$
t	Time
T	Gas temperature in the cavity
T_i	Gas temperature of incoming gas
T_{oil}	Oil temperature
v_s	Speed of sound in oil-gas mixture
v_d	Velocity in the discharge pipe
V	Cavity volume at instant t
V_i	Incoming volume flow rate
V_o	Outgoing volume flow rate
W	Work done by the system
ρ	Gas density in the cavity
ρ_i	Density of the incoming gas
ρ_{in}	Gas density at inlet conditions
ρ_{mix}	Gas density of the oil-gas mixture
α_m	Male rotor wrap angle in radians
θ	Male rotor rotation angle
ω	Angular velocity
ω_m	Male rotor angular velocity
ω_f	Female rotor angular velocity
γ	Specific heat ratio
Φ_d	Power used up by shear losses
μ	Oil viscosity
1,2	Subscripts for upstream, downstream condition
Σ	Summation over subscript i

Inlet and Discharge losses

Inlet losses:

Pressure drop in upstream restriction =

$$K_3 \frac{\rho_{in}}{2} \left(\frac{Q_f}{A_{min}}\right)^2$$

Centrifugal pressure deficit =

$$K_2 \frac{\rho_{in}}{32} \{\omega_m^2 (D_m^2 - D_{im}^2) + \omega_f^2 (D_f^2 - D_{if}^2)\}$$

Pressure Drop due to axial acceleration =

$$K_1 \frac{\rho_{in}}{2} \left\{\frac{\omega_m L}{\alpha_m}\right\}^2$$

Pressure Drop due to radial acceleration =

$$K_o \frac{\rho_{in}}{16} \{\omega_m^2 D_m^2 + \omega_f^2 D_f^2\}$$

Discharge 'acoustic' pressure increase =

$$K_4 \rho_{mix} v_s v_d$$

Rotor Tip Power Loss =

$$K_5 \mu \frac{\{\omega_m^2 D_m^2 A_{mt} + \omega_f^2 D_f^2 A_{ft}\}}{4 h_{rt}}$$

End Wall Power Loss =

$$K_6 \mu \pi \frac{\{\omega_m^2 (D_m^4 - D_{sm}^4) + \omega_f^2 (D_f^4 - D_{sf}^4)\}}{h_{ew}}$$

Interlobe shear loss =

$$K_7 \frac{\mu \omega_m^2 LR^3}{h_{il}}$$

REFERENCES

1. Singh, P.J. and Onuschak, A., "A Comprehensive Computerized Method For Twin-Screw Rotor Profile Generation and Analysis", International Compressor Engineering Conference, Purdue University, 1984.

2. Firnhaber, M.A., and Szarkowicz, D.S., "Modeling and Simulation of Rotary Screw Compressors", Purdue Compressor Technology Conference, 1980.

3. Brablik, J., "Analytical Model of an Oil-Free Screw Compressor", Purdue Compressor Technology Conference, 1982.

4. Sangfors, B., "Analytical Modeling of Helical Screw Machine for Analysis and Performance Prediction", Purdue Compressor Technology Conference, 1982.

5. Margolis, D.L., "Analytical Modeling of Helical Screw Turbines for Performance Prediction", ASME Journal of Engineering for Power, Vol. 100, July 1978.

6. Peterson, C.R. and McGahan, W.A., "Thermodynamic and Aerodynamic Analysis Method for Oil Flooded Sliding Vane Compressor", Purdue Compressor Technology Conference, 1972.